17th World Conference on Earthquake Engineering, 17WCEE

Sendai, Japan - September 13th to 18th 2020

A SPECTRAL ELEMENT METHOD FOR SEISMIC RESPONSE ANALYSIS OF SKELETAL STRUCTURES

Hongjing Li [1], Lu Han[2], Guangjun Sun [3]

[1] *Professor, Engineering Mechanics Institute, Nanjing Tech University, hjing@njtech.edu.cn*
[2] *Master candidate, Engineering Mechanics Institute, Nanjing Tech University, hanlu920@qq.com*
[3] *Associate professor, College of Civil Engineering, Nanjing Tech University, guangjunsun@njtech.edu.cn*

Abstract

The spectral element (SE) method, which combines the fast convergence of the spectral method with the well-adaptability of the finite element method, and owns low numerical dispersion and dissipation, has been developed recently as a potential numerical method to solve partial differential equations. However, the application of SE method in static and dynamic analysis of structures is seriously restricted by the lack of suitable SE model at present. In this paper, we develop a SE model of beam based upon the basic assumption of Bernoulli-Euler beam. The SE model of Bernoulli-Euler beam contains 5 nodes, consisting of 2 terminal nodes and 3 internal nodes. Total 12 degrees-of-freedom are considered within each element, namely axial, transverse and rotational degree-of-freedom for the terminal nodes but only axial and transverse degree-of-freedom for the internal nodes. According to the axial and transverse deformation of the beam, different interpolation modes are adopted independently. The characteristic matrices of spectral element are established by using Gauss-Lobatto-Legendre numerical integration quadrature, and the equivalent nodal force formula of spectral element are given. The numerical integration points are selected to be consistent with the arrangement of nodes of the beam element, so that mass matrix with diagonal form could be obtained. The beam's SE model appears to the C_1 element due to continuities of both deflection and rotation which can be manifested into the derivative of the deflection in Bernoulli-Euler beam theory. The beam's SE model can be conveniently applied to seismic response analysis of structures as the traditional finite element method. The numerical analysis results show that the beam's spectral element model can obtain high accuracy, and only one spectral element is needed for each component of the skeletal structures to achieve the desirable results.

Keywords: spectral element model, seismic response analysis, skeletal structures, GLL quadrature, C_1 continuity

1. Introduction

Seismic response analysis is the basic task for design and upgrade of seismic structures. There may be various methods of discretization to formulate the differential equations governing response of the structural systems subjected to earthquake induced ground motion. Recently, the spectral element method (SEM), which is gradually emerging as a numerical solution technique for the differential equation, has developed rapidly and become a powerful tool for the problems of physical and engineering sciences. The SEM combines the pseudo-spectral method (PSM) and the finite element method (FEM), and constructs the high-order element models by the technique of spectral expansion approximation. Therefore, the SEM features both "infinite order" convergence rate of the spectral method and flexibility and regularity of the FEM, but overcomes the shortcomings of the traditional high-order methods of the finite element model. Compare with the FEM, the SEM is applied rarely in the field of structural mechanics at present, owing to lack of spectral element model suitable to physical characteristics of the structural systems.

The SEM was first proposed by Patera [1] to solve the fluid dynamics problem in 1984. Instead of frequency-domain SEM which requires the operation of Fourier's transform, two kinds of spectral element models, the Chebyshev SEM and the Legendre SEM, are developed in time domain. The efforts during early days were mainly devoted to the Chebyshev SEM, such as the pioneering work of Patera [1], the research and application by Seriani and collaborators [2-6]. The Chebyshev SEM is still the important method used in the simulation of fluid dynamics and elastic waves [7-9]. On the other hand, Komatitsch et al. [10-13] contribute to the development of Legendre SEM and successfully solved the large-scale simulation problems in the field of geophysics. They developed the large-scale computer programs, SPECFEM 2D and SPECFEM 3D, which greatly promoted the application of Legendre SEM in practical physical problems. Kudela et al. [14-16] and Ostachowicz et al. [17-18] studied the propagation of elastic waves in media by means of Legendre SEM and have carried out the work of structural damage identification on this basis. For structural mechanics problems, Doyle [19], Lee [20], Igawa et al. [21], Li et al. [22] tried to apply the SEM in static and dynamic analysis of structures, but all these works were based on the frequency-domain SEM or called Fourier SEM, which is the early developed method and scarely used at present. In term of structural dynamics, only spectral element models for Timoshenko beams is presented up to now [23-29]. These spectral element models consist of two terminal nodes and several internal nodes. The deflection and rotation angle at each node are considered as independent degrees of freedom, and the Lagrange interpolation basis function on GLL nodes is selected as the shape functions. Then the deflection and rotation angle at each node are interpolated and the element characteristic matrices can be obtained by Gauss-Lobatto integration rule. Obviously, the spectral element model of Timoshenko beam only guarantees the continuity of deflection and rotation angle at the end nodes, but does not guarantee that their first order derivatives exist and are continuous, so it is a C_0-type element. For Bernoulli-Euler Beam, the deflection and the section rotation angle are not independent, they are required not only the deflection at the terminal nodes but also the rotation angles (first derivative of deflection) to be continuous. Namely, the Bernoulli-Euler beam element model should be C_1-type element [30]. In practice, the skeletal structure is usually regarded as an assembly of Bernoulli-Euler beams rather than the Timoshenko beams. Thus, the spectral element model of Bernoulli-Euler beam is needed for dynamic response analysis of the skeletal systems.

The objective of this paper is to develop a C_1-type spectral element model which accords with the Bernoulli-Euler beam theory, and solve the problems of seismic response analysis of the skeletal structures which used widely in engineering practice.

2. A spectral element model for Bernoulli-Euler beam

2.1 Choice of element nodes and degrees-of-freedom

Consider a standard one-dimensional element defined in dimensionless local coordinates $\xi \in [-1, 1]$, as shown in Fig.1. Since the spectral element model is the high-order element, the element nodes in the Bernoulli-

Euler beam model should be composed of two terminal nodes and a set of internal nodes. Assuming that the number of element nodes is p (p≥3), which includs two terminal nodes and at least one internal node. All these element nodes are arranged at the locations of Gauss-Lobatto-Legendre (GLL) integral points, determined by the roots of the equation:

$$\left(1-\xi^2\right)R'_{p-1}\left(\xi\right)=0 \tag{1}$$

where $R'_{p-1}(\xi)$ denotes the first-order derivative of the Legendre polynomial of p-1 degree.

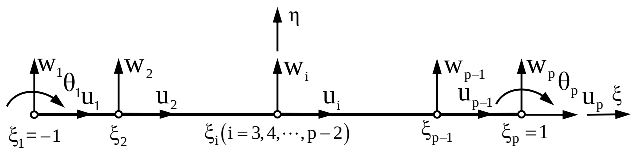

Fig. 1 – Spectral element model of Bernoulli-Euler beam

In general, each element node should contain three degrees of freedom (DOF), namely, deflection w, axial displacement u and rotation angle θ. According to basic assumption of Bernoulli-Euler beam, the rotation angle θ is the derivative of the deflection w, that is

$$\theta=\frac{dw}{dx}=\frac{2}{l^e}\cdot\frac{dw}{d\xi} \tag{2}$$

in which, l^e denotes the element length, x is the local coordinates, which has a transformation relationship with ξ as

$$\xi=\frac{2x}{l^e}-1 \quad \left(-1\le\xi\le 1\right) \tag{3}$$

Obviously, in order to construct the spectral element model with C_1 continuity, values of the derivatives of the field function must be continuous at the two terminal nodes. However, it is unnecessary to meet these requirements for the internal nodes because they are located within the same element. Therefore, the rotational DOFs at each internal node may be removed, and only DOFs of the deflection and axial displacement should be retained. As a result, total 2(p+1) DOFs should be contained in a spectral element model of the p-node Bernoulli-Euler beam, they are three DOFs for each terminal node and two DOFs for each internal nodes.

The order of the beam model mentioned above can reach at least p-1. We compare and analyze the spectral element models with different number of nodes. Based on a trade-off between the numerical accuracy and computational effort, the 5-node spectral element model is more appropriate and recommended.

2.2 Displacement function

In order to satisfy the condition of C_1 continuity, the axial displacements of u(ξ) and the deflections of w(ξ) within the spectral element are interpolated independently in different forms as

$$u\left(\xi\right)=\sum_{i=1}^{5}L_i\left(\xi\right)u_i \tag{4}$$

$$w\left(\xi\right)=\sum_{i=1}^{5}H_i\left(\xi\right)w_i+\hat{H}_1\left(\xi\right)\theta_1+\hat{H}_5\left(\xi\right)\theta_5 \tag{5}$$

where $u_i = u(\xi_i)$, $w_i = w(\xi_i)$ and $\theta_i = \theta(\xi_i)$ are the axial displacements, deflections and rotation angles at the GLL node coordinates of ξ_i (i=1, 2, …, 5), respectively. $L_i(\xi)$, $H_i(\xi)$ and $\hat{H}_i(\xi)$ denote the shape functions of the element, in which $L_i(\xi)$ can be designated by the Lagrange's interpolation formulation:

$$L_i(\xi) = \prod_{j=1, j\neq i}^{5} \frac{\xi - \xi_j}{\xi_i - \xi_j} \quad (i = 1, 2, \cdots, 5) \tag{6}$$

$H_i(\xi)$ and $\hat{H}_i(\xi)$ may be determined by the Hermite's interpolation polynomial, that is

$$H_i(\xi) = \begin{cases} \left(a_i\xi^2 + b_i\xi + c_i\right) L_i(\xi), & i = 1, 5 \\ \dfrac{\xi^2 - 1}{\xi_i^2 - 1} L_i(\xi), & i = 2, 3, 4 \end{cases} \tag{7}$$

$$\hat{H}_i(\xi) = \frac{1}{4}\xi_i l^e \left(\xi^2 - 1\right) L_i(\xi), \quad (i = 1, 5) \tag{8}$$

in which

$$a_i = -\frac{1 + 2\xi_i L_i'(\xi_i)}{4}, \; b_i = \frac{1}{2}\xi_i, \; c_i = \frac{3 + 2\xi_i L_i'(\xi_i)}{4}, \quad (i = 1, 5)$$

The displacement functions, u(ξ) and w(ξ), in Eqs.(4) and (5) are written uniformly in the matrix form:

$$\mathbf{u} = \mathbf{N}\delta^e \tag{9}$$

where

$$\mathbf{u} = \{u, w\}^T, \; \delta^e = \{\delta_1^e, \delta_2^e, \delta_3^e, \delta_4^e, \delta_5^e\}^T, \; \mathbf{N} = [\mathbf{N}_1, \mathbf{N}_2, \mathbf{N}_3, \mathbf{N}_4, \mathbf{N}_5]$$

Here defines that

$$\delta_i^e = \begin{cases} \{u_i, w_i, \theta_i\}, & i = 1, 5 \\ \{u_i, w_i\}, & i = 2, 3, 4 \end{cases}, \; \mathbf{N}_i = \begin{cases} \begin{bmatrix} L_i & 0 & 0 \\ 0 & H_i & \hat{H}_i \end{bmatrix}, & i = 1, 5 \\ \begin{bmatrix} L_i & 0 \\ 0 & H_i \end{bmatrix}, & i = 2, 3, 4 \end{cases}$$

2.3 Property matrices

The stiffness matrix and mass matrix could be derived for Galerkin weighted residual method, written as

$$\mathbf{K}^e = \int_{-1}^{1} \mathbf{B}^T \mathbf{D} \mathbf{B} |J| d\xi \tag{10}$$

$$\mathbf{M}^e = \int_{-1}^{1} \rho A \mathbf{N}^T \mathbf{N} |J| d\xi \tag{11}$$

in which ρ and A designate mass density per unit volume and cross-sectional area of the beam element, respectively; **B** is the element geometry matrix, which can be calculated by

$$\mathbf{B} = \Phi\mathbf{N} \tag{12}$$

where $\mathbf{\Phi}$ is a differential operator matrix, owning the following form:

$$\mathbf{\Phi} = \begin{bmatrix} \frac{\partial}{\partial x} & 0 \\ 0 & \frac{\partial^2}{\partial x^2} \end{bmatrix} \tag{13}$$

The elastic matrix of $\mathbf{D}$ is expressed as

$$\mathbf{D} = \begin{bmatrix} EA & 0 \\ 0 & EI \end{bmatrix} \tag{14}$$

where E and I present the Young's modulus and the moment of inertia of the beam section, respectively.

The Jacobi determinant of |J| in Eqs.(10) and (11) can be obtained by the coordinate transformation relation of Eq.(3), lead to

$$|J| = \frac{dx}{d\xi} = \frac{1}{2} l^e \tag{15}$$

In order to obtain the element stiffness matrix $\mathbf{K}^e$ and mass matrix $\mathbf{M}^e$, the GLL integration rule is introduced, that is, the integration in Eqs.(10) and (11) will be computed within the standard element of $\xi \in [-1, 1]$ as

$$\mathbf{K}^e \approx \frac{1}{2} l^e \sum_{i=1}^{5} \omega_i \mathbf{B}^T(\xi_i) \mathbf{D} \mathbf{B}(\xi_i) \tag{16}$$

$$\mathbf{M}^e \approx \frac{1}{2} \rho A l^e \sum_{i=1}^{5} \omega_i N^T(\xi_i) N(\xi_i) \tag{17}$$

in which ω_i is the integral weight coefficient.

2.4 Equivalent nodal forces

The equivalent nodal force vector of the beam element is written as

$$\mathbf{F}^e = \int_{\Omega} \mathbf{N}^T \mathbf{f} |J| d\xi \tag{18}$$

in which Ω is the distribution range of **f** designating the force vector of the element, denotes it as

$$\mathbf{f} = \{U(\xi), W(\xi)\}^T \tag{19}$$

where U(ξ) and W(ξ) are the axial and lateral distribution forces within the beam element, respectively.

The equivalent nodal forces are shown in Fig.2. Let them be in a vector:

$$\mathbf{F}^e = \{\mathbf{F}_1^e, \mathbf{F}_2^e, \mathbf{F}_3^e, \mathbf{F}_4^e, \mathbf{F}_5^e\}^T \tag{20}$$

in which

$$\mathbf{F}_i^e = \begin{cases} \{U_i, W_i, M_i\}, & i = 1, 5 \\ \{U_i, W_i\}, & i = 2, 3, 4 \end{cases}$$

where U_i, W_i and M_i represent the equivalent axial, lateral and bending moments of the element nodes, respectively.

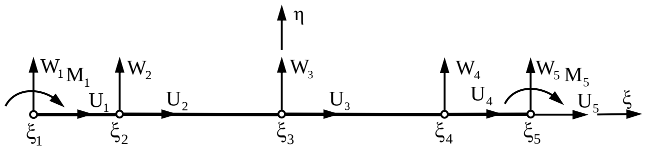

Fig. 2 – The equivalent nodal forces of the spectral element for Bernoulli-Euler Beam

2.5 Coordinate transformation

Both the property matrices and the equivalent nodal force vector are established above on the local coordinate, while the global coordinate description will be needed for analysis of the structural system, and this may be implemented by means of the coordinate transformation. Fig.3 and Fig.4 show the relationship between the local coordinate system of oxy and the global coordinate system of OXY for the equivalent nodal forces of the spectral element. Assume the angle between the two coordinate systems is α, which defined positive in counterclockwise rotation, then the equivalent nodal force vector in the global coordinate can be written as

$$\mathbf{F}^e = \mathbf{G}\tilde{\mathbf{F}}^e \tag{21}$$

in which $\tilde{\mathbf{F}}^e$ represents an array of element nodal forces in the global coordinates, $\mathbf{G}$ is the coordinate transformation matrix, which is expressed as

$$\mathbf{G} = \begin{bmatrix} \mathbf{G}_0 & & & & \\ & \mathbf{G}_1 & & & \\ & & \mathbf{G}_1 & & \\ & & & \mathbf{G}_1 & \\ & & & & \mathbf{G}_0 \end{bmatrix} \tag{22}$$

where

$$\mathbf{G}_0 = \begin{bmatrix} \cos\alpha & -\sin\alpha & 0 \\ -\sin\alpha & \cos\alpha & 0 \\ 0 & 0 & 1 \end{bmatrix}, \ \mathbf{G}_1 = \begin{bmatrix} \cos\alpha & -\sin\alpha \\ -\sin\alpha & \cos\alpha \end{bmatrix}$$

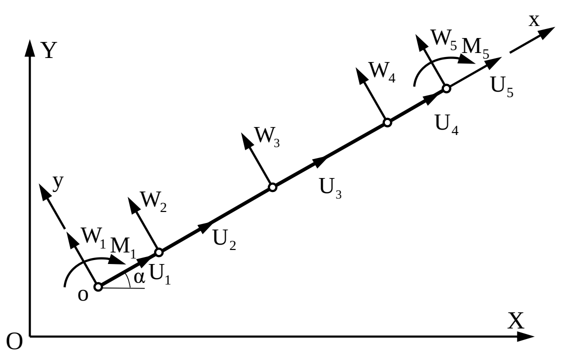

Fig. 3 – Nodal forces in the local coordinates

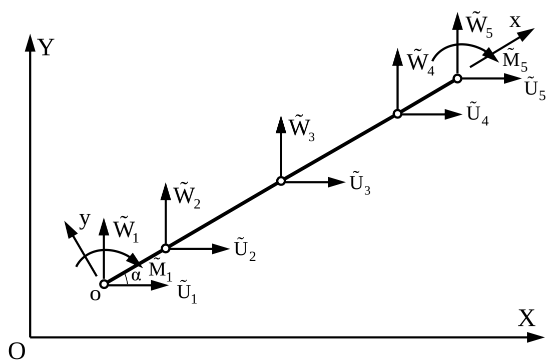

Fig. 4 – Nodal forces in the global coordinates

Noting that $\mathbf{G}$ is an orthogonal matrix, so $\tilde{\mathbf{F}}^e$ can be obtained by Eq.(21):

$$\tilde{\mathbf{F}}^e = \mathbf{G}^T \mathbf{F}^e \tag{23}$$

Accordingly, the element stiffness matrix and the mass matrix in the global coordinates can also be deduced as

$$\tilde{\mathbf{K}}^e = \mathbf{G}^T \mathbf{K}^e \mathbf{G} \tag{24}$$

$$\tilde{\mathbf{M}}^e = \mathbf{G}^T \mathbf{M}^e \mathbf{G} \tag{25}$$

3. Verification of the spectral element model

The convergence and the C_1 continuity of the 5-node spectral element model for Bernoulli-Euler beams are hereby verified by an example of simply supported beam, which resists uniformly distributed loads among the whole span, as shown in Fig.5. The corresponding parameters describing the beam are listed in Table 1.

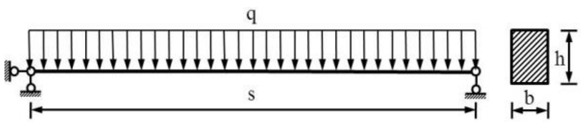

Fig. 5 – Simply supported beam

Table 1 – Parameters of simply supported beam

E(Pa)	s(m)	b(m)	h(m)	q(kN/m)
3.0×10^{10}	10.0	0.5	1.0	40.0

The simply supported beam is divided by m spectral elements with same length, and the cross-sectional rotation at x=0.0m and x=1.25m are measured and recorded as θ_0 and $\theta_{1.25}$, respectively, and the deflection at x=1.25m as $w_{1.25}$. The calculation results are listed in Table 2.

Table 2 – Comparison of structural response with different number of discrete spectral element

m	θ_0 ($\times10^{-3}$rad)	$\theta_{1.25}$ ($\times10^{-3}$rad)	$w_{1.25}$ ($\times10^{-3}$m)
1	1.33340	1.21884	-1.61795
2	1.33335	1.21877	-1.61786
3	1.33334	1.21876	-1.61785
4	1.33333	1.21875	-1.61784
Analytic solution	1.33333	1.21875	-1.61784

It can be seen from the calculation results in Table 2, that the response has been accurate enough even if only a spectral element is used for the simply supported beam. With increase of the number of spectral elements, the structural response can converge to the exact solution stably.

Next, the C_1 continuity of the spectral element model is examined. Take m=3, and the corresponding spectral elements are marked by ①, ② and ③, respectively, as shown in Fig.6. The responses of the terminal nodes which connect the adjacent spectral elements and are actually the common nodes for these elements are computed for each spectral element and listed in Table 3. One may find obviously that not only the field function (deflection) but also the first-order derivative of the field function (rotation angle) are continuous at the junction of the adjacent spectral elements, that is, the spectral element is a C_1-type element model.

Fig. 6 – Partition of spectral elements

Table 3 – C_1 continuity verification

Responses	**① left**	**② left**	**② right**	**③ left**
w($\times10^{-3}$m)	-3.62138	-3.62138	-3.62138	-3.62138
θ($\times10^{-3}$rad)	0.64198	0.64198	-0.64198	-0.64198

4. Application to the skeletal structures

4.1 Dynamic analysis

A portal frame shown in Fig.7 is selected as an example of the dynamic problem. Every component of the structure is simulated by one spectral element, so total 3 spectral elements have been employed for the portal frame. The spectral elements and the corresponding nodes used are numbered as shown in Fig.8. Assuming that all the elements are 10.0m length, and with a rectangular section of 0.5m×1.0m, an elastic modulus of $E=3.0\times10^{10}$ Pa, and a mass density per unit volume of $\rho=80t/m^3$. The lateral force acted on the structure is $F(t)=500\sin(\pi t)$ N.

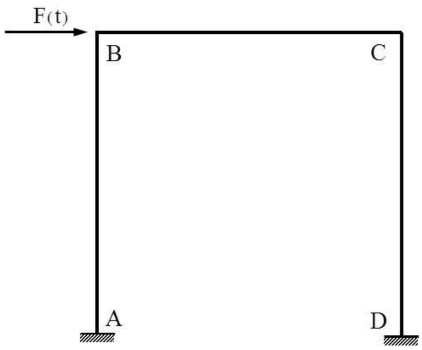

Fig. 7 – Example of the portal frame

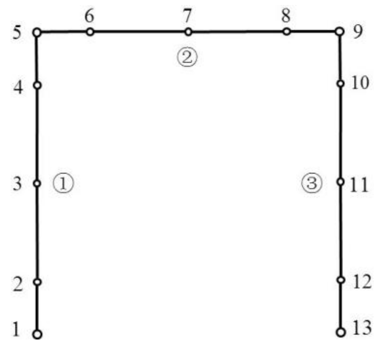

Fig. 8 – Numbered spectral elements and nodes

Obviously, the boundary conditions of the portal frame should be

$$u_1 = w_1 = \theta_1 = 0,\ u_{13} = w_{13} = \theta_{13} = 0$$

After the boundary conditions are treated, the global mass matrix of the portal frame can be written as

$$\mathbf{M} = \begin{bmatrix} \mathbf{M}_2 & & & \\ & \mathbf{M}_3 & & \\ & & \ddots & \\ & & & \mathbf{M}_{12} \end{bmatrix} \qquad (26)$$

in which

$$M_i = \begin{bmatrix} m_i^x & \\ & m_i^y \end{bmatrix} \text{ for i=2,3,4,6,7,8,10,11,12}$$

and

$$M_i = \begin{bmatrix} m_i^x & & \\ & m_i^y & \\ & & 0 \end{bmatrix} \text{ for i=5,9}$$

where m_i^x and m_i^y denote the mass of node i in the x and y directions, respectively. The mass matrix of the spectral element is calculated according to Eq.(17) and Eq.(25), then the whole mass matrix is integrated.

It is noted that the masses corresponding to node 5 and 9, the rotational degrees of freedom, is zero in the global mass matrix, this is the result of the basic assumption of Bernoulli-Euler beam. Static condensation technique can be used to eliminate the two rotational degrees of freedom in dynamic analysis.

Based on the spectral element model, the first five natural frequencies of the frame are calculated and listed Table 4. The reference solutions in the table are the results computed by the general finite element software, while SEM1 and SEM2 present the solutions in which the mass matrix has and has not processed by the static condensation technique, respectively.

Table 4 – Calculation results of the natural frequencies (unit: rad/s)

Mode	**SEM1**	**SEM2**	**Reference solution**
1	5.6528	5.6528	5.6538
2	21.9255	21.9255	21.9469
3	36.2182	36.2182	36.3926
4	37.7287	37.7287	38.0269
5	69.9744	69.9744	68.3921

According to Eq.(26), although the mass matrix **M** in this example is singular, it does not affect the natural frequency analysis. It can be seen from Table 4 that the rotational degrees of freedom has little influence on the natural characteristics, this also shows reasonability of the basic assumption of Bernoulli-Euler beam.

In order to verify the dynamic response, the step-by-step integration procedure is used to the portal frame above. The time history of lateral displacement response at point B is given in Fig.9, comparing with the reference solution. It is found that the spectral element model can still achieve high accuracy in solving dynamic problems.

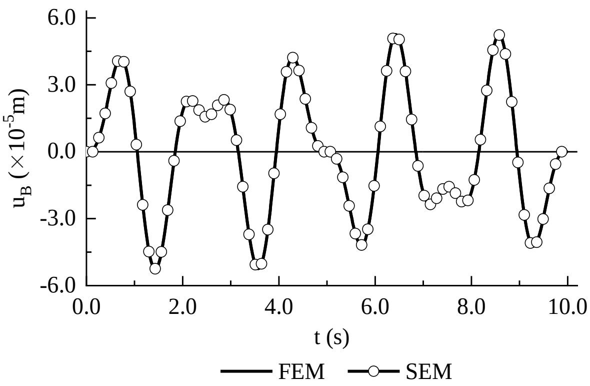

Fig. 9 – Time history of lateral displacement response at point B

4.2 Seismic response analysis

Assuming the portal frame above is excited by earthquake-induced ground motion, and time-history response of the lateral displacement at point B is calculated with the 5-node spectral element model for examination. Two strong-motion accelerograms recorded respectively during the Imperial Valley earthquake of 1940 and the Parkfield earthquake of 1966 are selected for analysis of structural dynamics. These two recorded ground motions are shown in Fig.10 and Fig.11.

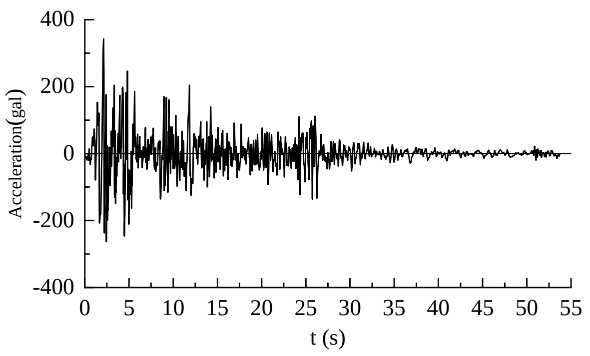

Fig. 10 – Ground motion, El Centro 1940

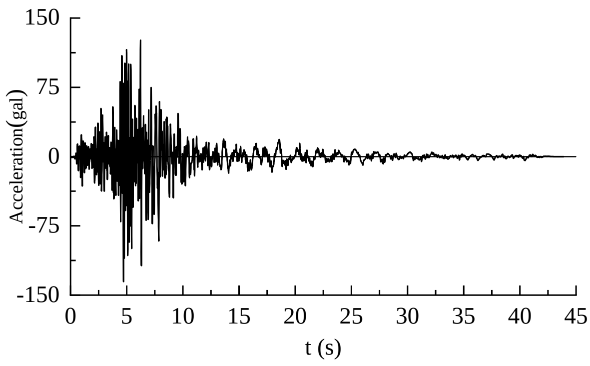

Fig. 11 – Ground motion, Cholame 1966

The seismic response of the lateral displacement at point B to the two ground motions are shown in Fig.12 and Fig.13, respectively. Only first 30 seconds of the duration are extracted out, and reference solutions computed by the general finite element software under the same circumstance for comparison.

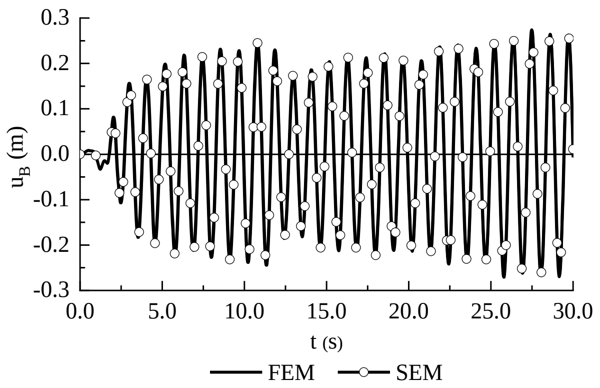

Fig. 12 – Response to El Centro excitation

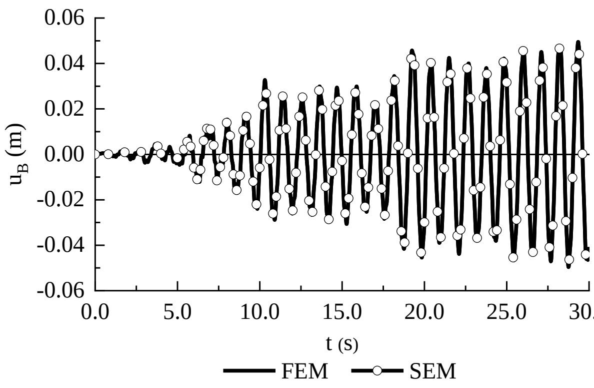

Fig. 13 – Response to Cholame excitation

As one has seen from the diagrams, the resulting responses acquired by the spectral element model are in good accordance with the reference solution, and the spectral element model can still achieve high accuracy in solving seismic analysis problems.

5. Conclusions

Based on the Bernoulli-Euler Beam theory, a spectral element model which can be directly applied to the dynamic analysis of skeletal structures is developed in this paper, the main conclusions are as follows:

(1) The 5-node beam spectral element model developed in this paper can not only ensure the continuity of displacement at the junction of the element, but also effectively ensure the continuity of section normal before deformation at the junction. Therefore, the spectral element model of the beam accords with the basic assumption of Bernoulli-Euler beam and satisfies the C_1 continuity requirement.

(2) For the axial displacement and deflection of the beam, different interpolation modes are used to simulate the field functions of axial and transverse deformation independently, which is a reasonable way to

realize the basic assumption of Bernoulli-Euler beam. The main mechanical properties of Bernoulli-Euler beam can be manifested through the spectral element model.

(3) The order of the element field function is effectively reduced by removing the rotational degrees of freedom of the sections at the three internal nodes within the beam spectral element model. The Legendre spectral element method can obtain the element property matrix accurately enough by GLL integration rule. Numerical experiments show that the spectral element model without internal nodal rotational degrees of freedom can gain high numerical accuracy, and the section rotation angle can be accurately obtained by derivation of the deflection interpolation function.

(4) The spectral element model of beam can be conveniently applied to the dynamic analysis of skeletal structures. Because of the high accuracy of spectral element method, the results of ordinary system may be calculated accurately by dividing each component into one spectral element.

Acknowledgements

The authors would like to acknowledge the partial support provided by the National Natural Science Foundation of China under Grant Number of 51478222.

References

[1] Patera AT (1984): A spectral element method for fluid dynamics: laminar flow in a channel expansion. *Journal of Computational Physics*, **54** (3), 468-488.

[2] Seriani G, Priolo E, Carcione J, Padovani E (1992): High-order spectral element method for elastic wave modeling. *SEG Technical Program Expanded Abstracts*.

[3] Seriani G, Priolo E (1994): Spectral element method for acoustic wave simulation in heterogeneous media. *Finite Elements in Analysis and Design*, **16** (3-4), 337-348.

[4] Padovani E, Priolo E, Seriani G (1994): Low and high order finite element method: experience in seismic modelling. *Journal of Computational Acoustics*, **2** (4), 371-422.

[5] Priolo E, Carcione JM, Seriani G (1994): Numerical simulation of interface waves by high-order spectral modeling techniques. *The Journal of the Acoustical Society of America*, **95** (2), 681-693.

[6] Dauksher W, Emery AF (1997): Accuracy in modeling the acoustic wave equation with Chebyshev spectral finite elements. *Finite Elements in Analysis and Design*, **26** (2), 115-128.

[7] Karniadakis GE, Sherwin S (2005). *Spectral/hp element methods for computational fluid dynamics*. Oxford University Press, 2nd edition.

[8] Lin W, Wang X, Zhang H (2005): Spectral element method based on element-by-element technique for elastic wave equation simulation. *Progress in Natural Science*, **15** (9), 1048-1057.

[9] Wang X, Seriani G, Lin W (2007): Some theoretical problems of calculating elastic wave field by spectral element method. *Scientia Sinica Series G*, **37** (1), 41-59.

[10] Komatitsch D, Vilotte JP (1998): The spectral element method: an efficient tool to simulate the seismic response of 2D and 3D geological structures. *Bulletin of the Seismological Society America*, **88** (2), 368-392.

[11] Komatitsch D, Vilotte JP, Vai R, Castillo-Covarrubias JM, Sanchez-Sesma FJ (1999): The spectral element method for elastic wave equations—application to 2-D and 3-D seismic problems. *International Journal for Numerical Methods in Engineering*, **45** (9), 1139-1164.

[12] Komatitsch D, Tromp J (1999): Introduction to the spectral element method for three-dimensional seismic wave propagation. *Geophysical Journal International*, **139** (3), 806-822.

[13] Komatitsch D, Martin R, Tromp J, Taylor MA, Wingate BA (2001): Wave propagation in 2-D elastic media using a spectral element method with triangles and quadrangles. *Journal of Computational Acoustics*, **9** (2), 703-718.

[14] Kudela P, Krawczuk M, Ostachowicz W (2007): Wave propagation modelling in 1D structures using spectral finite elements. *Journal of Sound and Vibration*, **300** (1-2), 88-100.

[15] Kudela P, Żak A, Krawczuk M, Ostachowicz W (2007): Modelling of wave propagation in composite plates using the time domain spectral element method. *Journal of Sound and Vibration*, **302** (4-5), 728-745.

[16] Kudela P, Ostachowicz W (2009): 3D time-domain spectral elements for stress waves modeling. *Journal of Physics: Conference Series*, **181** (1), 012091.

[17] Ostachowicz W, Kudela P (2010): Wave propagation numerical models in damage detection based on the time domain spectral element method. *IOP Conference Series: Materials Science and Engineering*, **10** (1), 012068.

[18] Ostachowicz W, Kudela P, Krawczuk M, Żak A (2011): *Guided waves in structures for SHM: the time-domain spectral element method*. John Wiley & Sons, Ltd.

[19] Doyle JF (1997): *Wave propagation in structures: spectral analysis using fast discrete Fourier transforms*. Springer, 2nd edition.

[20] Lee U (2009): *Spectral element method in structural dynamics*. John Wiley & Sons (Asia) Pte Ltd.

[21] Igawa H, Komatsu K, Yamaguchi I, Kasai T. (2004): Wave propagation analysis of frame structures using the spectral element method. *Journal of Sound and Vibration*, **277** (4), 1071-1081.

[22] Li FM, Liu CC (2015): Vibration analysis and active control for frame structures with piezoelectric rods using spectral element method. *Archive of Applied Mechanics*, **85** (5), 675-690.

[23] Lee U, Lee C (2009): Spectral element modeling for extended Timoshenko beams. *Journal of Sound and Vibration*, **319** (3-5), 993-1002.

[24] Lee U, Jang I (2010): Spectral element model for axially loaded bending-shear-torsion coupled composite Timoshenko beams. *Composite Structures*, **92** (12), 2860-2870.

[25] Lee U, Kim D, Park I (2013): Dynamic modeling and analysis of the PZT-bonded composite Timoshenko beams: spectral element method. *Journal of Sound and Vibration*, **332** (6), 1585-1609.

[26] Jang I, Park I, Lee U (2014): Guided waves in a Timoshenko beam with a bonded composite patch: frequency domain spectral element modeling and analysis. *Composites Part B: Engineering*, **60**, 248-260.

[27] Song Y, Kim S, Park I, Lee U. (2015): Dynamics of two-layer smart composite Timoshenko beams: frequency domain spectral element analysis. *Thin-Walled Structures*, **89**, 84-92.

[28] Żak A, Krawczuk M, Palacz M, Doliński Ł, Waszkowiak W. (2017): High frequency dynamics of an isotropic Timoshenko periodic beam by the use of the time-domain spectral finite element method. *Journal of Sound and Vibration*, **409**, 318-335.

[29] Sarvestan V, Mirdamadi HR, Ghayour M (2017): Vibration analysis of cracked Timoshenko beam under moving load with constant velocity and acceleration by spectral finite element method. *International Journal of Mechanical Sciences*, **122**, 318-330.

[30] Zienkiewicz OC, Taylor RL, Zhu JZ (2013): *The finite element method: its basis and fundamentals*. Elsevier Ltd., 7th edition.

